ORIGINAL ARTICLE

Vibrational study of benzalkonium chloride (1) interaction with metallic ions and surfaces: surface enhanced Raman spectroscopy study of (1) with human serum albumin

MC Álvarez-Ros, PhD

Álvarez-Ros MC. Vibrational study of benzalkonium chloride (1) interaction with metallic ions and surfaces: surface enhanced Raman spectroscopy study of (1) with human serum albumin. J Pharm Toxicol. 2018;1(2):14-9

In this paper Raman Spectroscopy is used to study the interaction of microbicide N-Alkyl-N, N-dimethyl-N-benzylammonium chloride (Benzalkonium Chloride or Barquat–80) with metallic ions. The technique Surface Enhanced Raman Scattering applies to this purpose. This technique applies to the study of the interaction of this compound with Human Serum Albumin (HSA). The observed changes in the spectrum indicate that the alkane chain and the – CH_3 or - CH_2 radicals of barquat attack HAS and the interaction with HSA and Barquat is on the aromatic ring too. Very important features of benzalkonium salts are their bactericidal and antimicrobial properties.

Key Words: *Raman spectroscopy; Human serum albumin; Benzalkonium salts*

Barquat–80 (B–80), a quaternary ammonium compound (QAC), is an effective microbicide, fungicide, deodorant and algicide used in general disinfection and general sanitizing. It´s handed containing approximately 7 % isopropanol and approximately 13% water. The molecule shows a no fixed structure (Figure 1) and the average molecular weight is 364 (1).

Quaternary ammonium compounds are a group of excellent antimicrobial activity, they are mainly used as disinfectant, biocide, and detergent, but also as anti-electrostatic, and very important features of benzalkonium salts are their bactericidal and antimicrobial properties. They are widely used as preservative for ophthalmic, nasal and parenteral products and as topical antiseptics and disinfectants for medical equipment (2). There are studies about the application of Barquat–80 in ocular medicine (3,4) in ophthalmology (5-7) and about several independent decellularization protocols on (porcine) cornea for future clinical use (8) and as cross-linker agents in dentist medicine (9) and are evaluated its bactericidal activity against several bacteria (10-12) and an method was developed for assay determination of Benzalkonium chloride (BKC) in nasal spray formulations (13). Benzalkonium salts (chloride and bromide) inhibit the proliferation of a variety of cells and are effective bactericidal, fungicidal and virucidal agents. They show inhibitor activity against many pathogens virus including human immunodeficiency virus (HIV) and are useful in prevention and treatment of other diseases mainly those originated by viruses and at the skin surface (14) and there are studies about biodegradation of quaternary ammonium compounds (15).

The misuses of QAC, can lead to increasing resistance of microorganisms. For to avoid this serious problem it is suitable the use of new biocides with modified structures instead of the biocides applied so far. New BAC analogues P13–P18 with pyridine rings were synthetized. The new compounds were characterized by NMR, FT-IR and ESI-MS methods. Several features as critical micellization concentrations and antimicrobial properties of novel QACs were examined by determining their minimal inhibitory concentration (MIC) values against several bacteria (16) and there are studies about the biological and medical behavior of BCK (17-19), about the synthesis and biological properties (20) and as preservative used most commonly in eye drops. There are studies that have demonstrated adverse effects on surface epithelial cells for the extend use in eye drops and to decrease in corneal damages by addition of several protective medical substances (7,21-26). BCK could favor drug release in therapies that requires faster but controlled delivery (27). We thing that it is important to study the interaction between this molecule and metallic ions because possible arrive, as waste, to environment and may act with metallic ions that are present. In this way, at the beginning, we have studied the FT-Raman spectrum of this molecule and Surface Enhanced Raman Spectroscopy (SERS) over silver colloids and over mixed silver and magnetic colloids. SERS is a technique that obtains a very increase in the intensity of the Raman signal of a molecule physical or chemical absorbed on a rough metal surface whose size is microscopic particle. When an electromagnetic wave interacts with metal surface, that the fields next this surface change in regard the far field and if it is rough, the plasmons on the surface get turned on and the electromagnetic field is amplified (28-30). This technique is widely used for study the molecules absorbed on metallic surfaces mainly in colloids of silver or copper. SERS allows obtain spectra of substances at very low concentration (31,32). Two theories explain this technique: The electromagnetic theory relies upon the excitation of localized surface plasmons and the chemical theory explains the effect through the formation of charge – transfer complexes (33). At present there are several studies about the SERS enhancement factor of silver sphere nanoparticles depended on temperature (34) and there are recent reviews on the manufacture of SERS substrates and the requirements for characterization of plasmonic materials as SERS platforms (35). Studies about the synthesis of gold nanoparticles are proposed, an instantaneously method using non-toxic reducing agents and applied to SERS (36).

Recent developments have been made concerning the fabrication of 3D SERS-active hot spot and fabrication of novel 3D plasmonic nanostructures (37). The serum albumins belong to a multigene family of proteins that are of use in the transport, distribution, and metabolism of many endogenous and exogenous ligands: molecules of fatty acids, metals as calcium, zinc and copper, amino acids, hormones, steroids and numerous of therapeutic drugs. Albumins are characterized by a low reserved of tryptophan and methionine and a high content in cystine and charged amino acids. The feature of the albumin molecule is a series of nine loops that repeat in a triplet fashion of large-small-large loops and further grouped as three homologous domains of three loops every one. The three domains also consist of six subdomains. It is included the alignment of 17 disulfide bridges between cystine residue (38-42). The human serum albumin (HSA) (molecular weight 66.439 u.m.a. from composition) consist of 585 amino acids with 35 residues cysteine that form the disulfur bridges at the origin of its tertiary structure and shows a thiol grouping at the level of cysteine (34).

The albumin is the more abundant protein of the plasma, about 60% (43) and plays a key role in transport, distribution and metabolism of metabolites and drugs (44). Recombinant human serum albumin (rHSA) is potential alternatives for human serum albumin (HSA) which may ease severe shortage of HSA worldwide. In theory, rHSA and HSA are the same and analysis

Department of Chemistry-Physics I, Faculty of Chemical Sciences, Complutense University, Ciudad Universitaria, Madrid, Spain

Correspondence: MC Álvarez-Ros, Department of Chemistry-Physics I, Faculty of Chemical Sciences, Complutense University, Ciudad Universitaria, Madrid, Spain. Telephone +34-913-944-272, e-mail maralva32@yahoo.es

Received: February 21, 2018, Accepted: April 18, 2018, Published: April 30, 2018

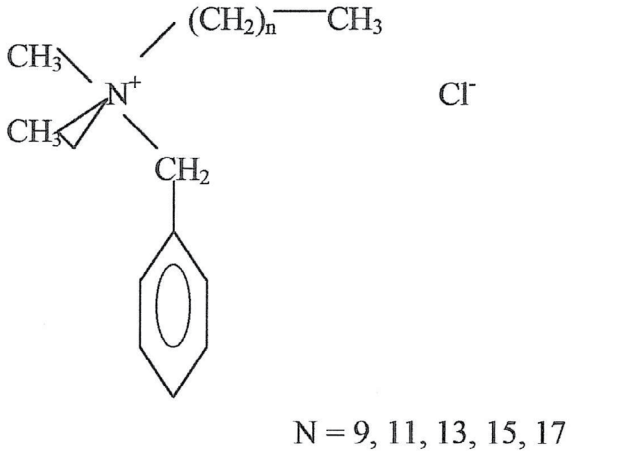

Figure 1) *N-Alkyl-N,N-dimethyl-N-benzylammonium chloride*

indicated that rHSA and HSA achieved a structural similarity of 99% (45).

The single tryptophan is at residue 214, in loop four. Distribution of other amino acids is uneven, tyrosine is in loops three and six and prolines are in the tip of each long loop. The molecule is not charged uniformly along his length, thus the charge is -9, -8 and +2 in domains I, II and III39.

In this study we have used a silver colloid (named as A), mixed colloid, Ag colloid + magnetic colloid (B) and C, silver colloid using hydroxylamine as reducing agent.

EXPERIMENTAL

Materials

All materials for prepare the colloids: $AgNO_3$, $FeCl_2$, $FeCl_3$, HNO_3, $NaC_6O_7H_8$ and NH_4OH, were purchased from Merck and also KNO_3, NaCl in Riedle-De Haën AG and Na_2SO_4 from Fluka. HSA from Sigma Chemical Co. (Seelze, Germany) and were used without further purification. All were in grade of purity for analysis. The water solutions were prepared with triply distilled water. Barquat–80 was get in Lonza group.

Preparation of colloids

Silver colloid (A) was prepared by Lee method (46): To 50 ml of boiling $AgNO_3$ aqueous solution 10^{-3} M, vigorously stirred, are added 1 ml of aqueous sodium citrate (1%), drop by drop and remain boiling and stirring during one hour. Magnetic colloid was prepared by Massart method (47) a little modified: A mix that consist of 10 ml of $FeCl_3$ aqueous solution, 1 M and 2.5 ml of $FeCl_2$ 2 M dissolved in HCl 2 M was added drop by drop to 125 ml of NH_4OH 0.7 M and it was vigorously stirred. A solid precipitate of Fe_3O_4 is obtained that is washed with HNO_3 2 M. This solid is separated by means of a centrifuge and abundant triply distilled water is added for obtain the peptization. Mixed colloids were prepared dissolving solid $AgNO_3$ into 50 ml of aqueous solution of magnetic colloid at calculated concentration and, when it is boiling, 1 ml of sodium citrate was added at 1% of concentration. We have named as B colloid. The silver colloid using hydroxylamine as reducing, named C colloid, was prepared by Lendl and method (48), that consist of dissolve 0.017 g of $AgNO_3$ in 90 ml of triply distilled water, also 0.021 g of NH_3OHCl are added to 5 ml of water and 4.5 ml of NaOH 0.1 M also are added. All this mixture is emptied quickly and stirring on $AgNO_3$ solution.

Instrumentation

The absorption spectrum recorded with a double beam Cintra 5 UV visible absorption spectrophotometer using a 10 mm silica cell. FT-Raman spectrum was recorded with Bruker RFS 100/S by using a ND: YAG laser source at 1064 nm, the output power was 150 mW. The sample was placed into a 10 mm silica cell. The final spectrums were the result of 1000 scans accumulations and power about 300 mW. Raman spectrum was recorded with a Renishaw R.M. 1000 by using a laser source at 782 nm and placing the liquid sample on a glass sheet and evaporating until obtain a solid residue and objective 100. We have obtained also microscopic pictures of internal structure of samples.

DISCUSSION

Absorption spectra of pure Barquat CB–80 and 10^{-5} M over (A) and © colloid

We have gotten the absorption spectrum of Barquat 80% and pH=5.0 at 10% of dilution, that shows one peak at 215 nm and a shoulder about 257 nm that disappears in solution. The spectra of Barquat at concentration 10^{-5} M and on (A) colloid and pH=5.3; on (C) colloid containing 0.1% of magnetic colloid and pH=5.0; on (C) colloid containing 0.5% of magnetic colloid and on (C) colloid containing 1% of magnetic colloid and pH=4.7 only show a highest value about 200 nm. These indicate the interaction with the metal of colloid. The spectrum is not visible at as low concentration 10^{-5} M.

FT-Raman spectra of Barquat CB-80 and SERS

In the Table 1, are indicated the possible main vibrations frequencies of FT-Raman spectrum of Barquat-80 and FT-SERS of aqueous solution 10^{-5} M × 10 over A colloid and over mixed colloid (B) 1% and Raman spectrum on Ag colloid (C). The mixed colloid formed for silver colloid over 1% of magnetic colloid contains particles of Fe_3O_4 recovered of particles of silver that present interaction with the light. This fact pointed that both spectra, over silver colloid (A) and over mixed colloid (B), present few differences and had been our object of study in older works. It´s observed that the strong band, in the spectrum of alone Barquat, at 2891 cm^{-1}, is not present in the other three spectra and the very strong band at 2852 cm^{-1} appears as a shoulder at 2848 cm^{-1} in SERS over silver colloid and at 2856 cm^{-1} in SERS over mixed colloid and on C colloid do not appear. Both bands correspond to $-CH_2$ symmetric stretching, that is to say, that are corresponding to paraffin chains. The bands at 1004 and 1032 cm^{-1}, corresponding to aromatic chain, appear practically equal in FT-SERS on A and B colloids that in alone Barquat, only change the intensity, but on C colloid the intensity does not change. In the two first peaks, the intensity decreases in FT-SERS on Ag colloid and in FT-SERS of mixed colloid and, in Raman spectra on Ag colloid, the intensity do not change but the peaks are little shifted (at 1039 cm^{-1} and 1003 cm^{-1}, respectively). The shoulder at 2931 cm^{-1}, corresponding to $-CH_3$ anti-symmetric stretching, appears strong in FT-SERS on Ag colloid and medium 2938 cm^{-1} in FT-SERS on mixed colloid and in Raman spectra on Ag colloid do not appears. The strong peak at 1448 cm^{-1}, also corresponding to $-CH_3$ anti-symmetric, changes the intensity and, on C colloid, the band is about 1456-1453 cm^{-1}. The medium peak at 1302 cm^{-1} in alone barquat-80, possible to –CH methane deformation, changes the intensity and lightly its value and the band at 873-888 cm^{-1}, only appears in spectrum on C colloid. As we stated in the previous paragraph, Barquat shows an N+ linked to an aromatic radical and also linked to two $-CH_3$ groups and to a very long paraffin chain, which has from 10 to 18 carbon atoms. It makes the union of this positive nitrogen with the negative surface formed for the citrate anion, which recover the metallic atoms of silver, guides the long paraffin chain far away of the negative surface, due to stereo reason, and $-CH_3$ groups and aromatic chain are located next to the surface. This fact is the reason of the weak bands corresponding to paraffinic chain.

FT-Raman of SERS of Barquat–80 over silver colloid (A) after addition of NaCl, KNO_3 and Na_2SO_4

The Figure 2 displays SERS of Barquat–80 over silver colloid (A) at concentration 10^{-5} M and pH=5.3: a) alone; b) with NaCl 10^{-2} M; c) with KNO_3 10^{-2} M and d) with Na_2SO_4 10^{-2} M. All these compounds increase the profile of spectra. It´s observed that the larger increase appears for addition of NaCl and it is possible, due to interaction between Cl^- anion and Ag^+ forming a larger negative sheet over the surface, that fixed more intense the N^+.

We have studied FT-Raman SERS of Barquat of 10^{-5} M over (A) colloid with Na_2SO_4 10^{-2} M and over (C) colloid with Na_2SO_4 10^{-1} M (Figure 3). The spectrum over © colloid, obtained using Na_2SO_4 as gathering substance, shows more intense that on (A) colloid. The main bands are the same in both spectra but the spectrum on A colloid shows the peaks at 1324 and 1386 cm^{-1} appointed to vibrations of benzene more intense that on C colloid.

SERS of albumin + barquat over (A) colloid

Table 2 shows Raman SERS of Albumin 2.8×10^{-5} M + KNO_3 3×10^{-3} M (x5), barquat 7×10^{-6} M + KNO_3 3×10^{-3} M and albumin + Barquat 4/1 + KNO_3 3×10^{-3} M (x5). It is noted the main peaks of SERS of mixed albumin and Barquat in relation 4/1 and are compared with the SERS of albumin and Barquat at the same concentration, 2.8×10^{-5} M for albumin and 7×10^{-6} M for Barquat) and addition of KNO_3 3×10^{-3} M. In the Figure 4, it is mainly observed that the intensity of the spectrum of the mixture Albumin-Barquat

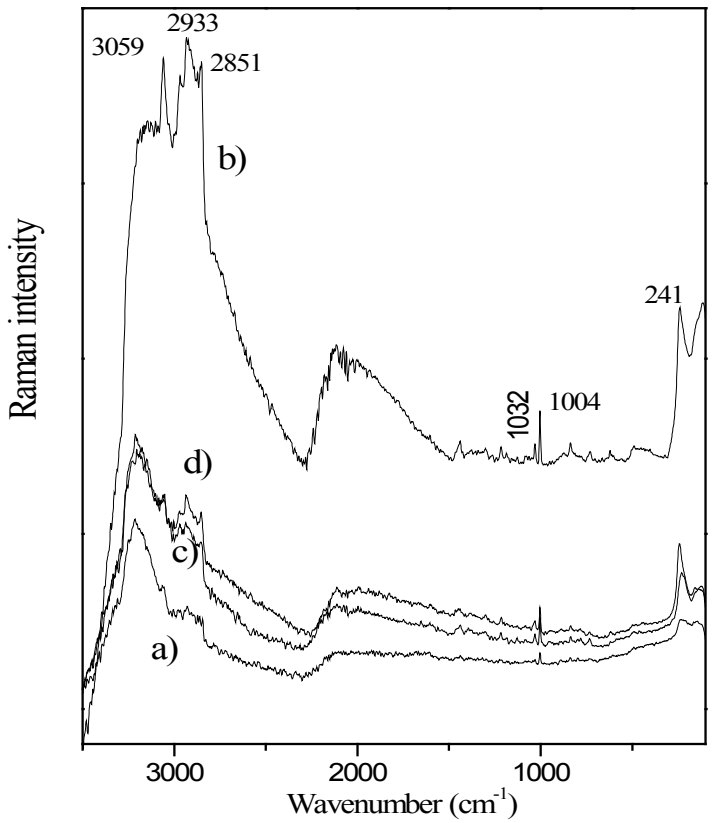

Figure 2) *FT-Raman SERS of Barquat 10^{-5} M over (A) colloid: a) alone; b) with NaCl 10^{-2} M; c) with KNO_3 10^{-2} M and d) with Na_2SO_4 10^{-2} M*

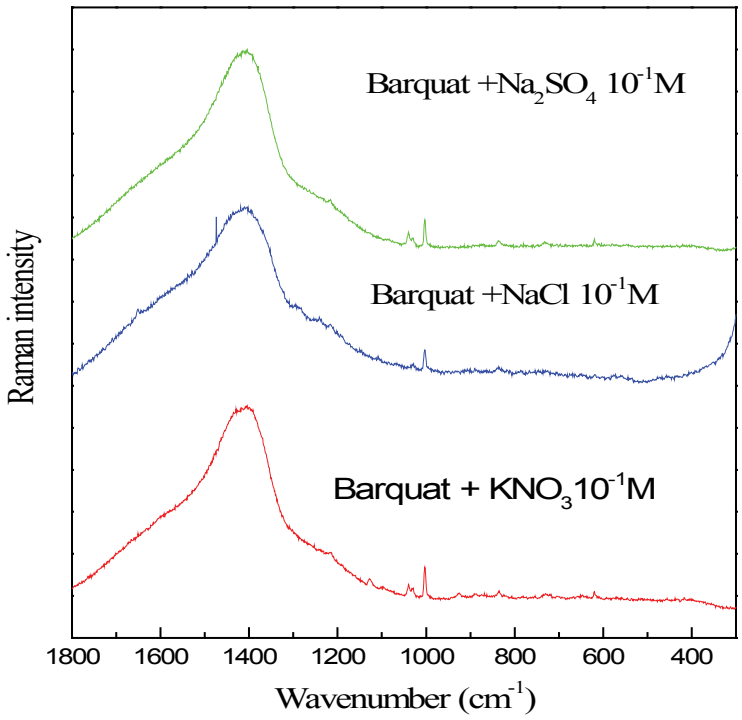

Figure 3) *SERS of Barquat (ac) 10^{-3} M on Ag colloid of hidroxilamine*

is lower that the intensity of alone Barquat (the spectrum of the mixture is multiplied by 5). Table 2 shows some differences in the peaks of alone Barquat in respect the mixture: the medium peak at 2926 cm^{-1} of Barquat appears strong in the mixture; the shoulder at 2892 cm^{-1} disappears in the mixture and it is noted that the weak band at 1382 cm^{-1}, corresponding to $-CH_3$ anti-symmetric deformation in alone Barquat, is observed strong at 1386 cm^{-1} in the mixture and joined to 1378 cm^{-1} in alone albumin and the peak of Barquat at 1127 cm^{-1}, corresponding to (-C-C-) alkane stretching or δ (CH) aromatic, decreases in the bands of the mixture. We think that these changes indicate that the alkane chain and the $-CH_3$ or $-CH_2$ radicals attach HAS. The aromatic peak, in Barquat, at 1604 cm^{-1}, is weaker in the mixture, the also aromatic weak peak at 1083 cm^{-1} in Barquat possible is at 1075 cm^{-1} with the same intensity in the mixture. It is also observed that the medium band at 831 cm^{-1} in albumin disappears or is strong at 837 cm^{-1}, joined to the point of alone Barquat and the peaks at 736 cm^{-1} (weak) in albumin, 734 cm^{-1}

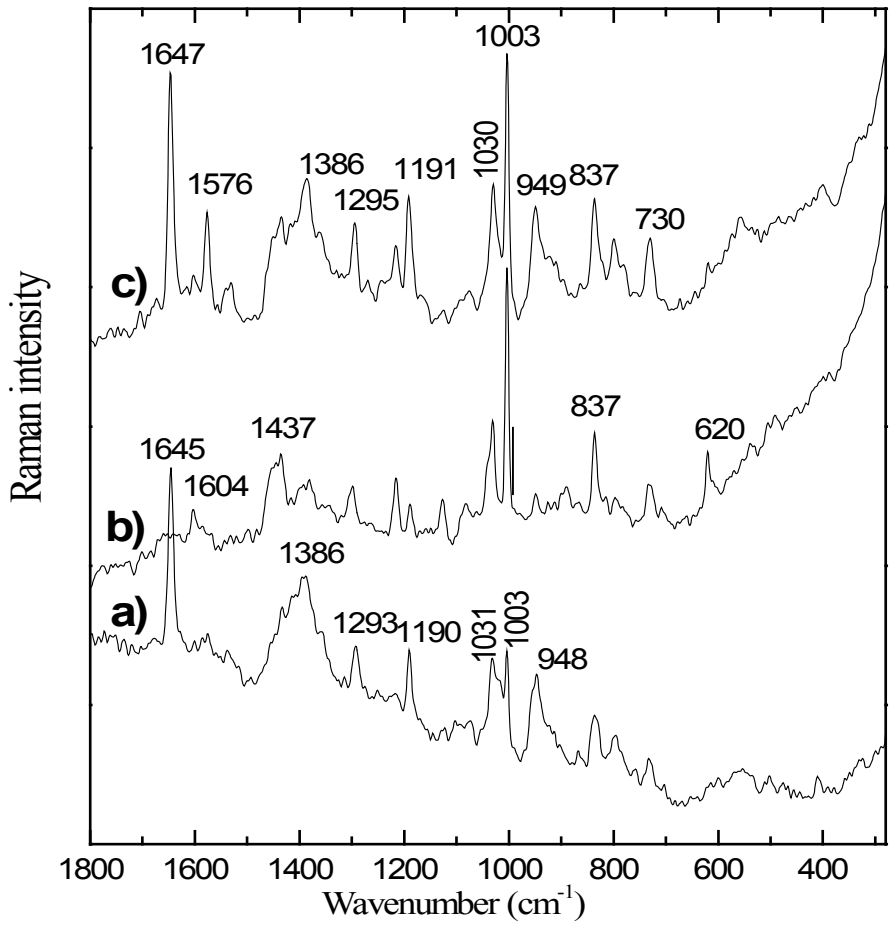

Figure 4) *Raman SERS: a) Albumin 2.8 × 10^{-5} M + KNO_3 3 × 10^{-3} M (x5); b) barquat 7 × 10^{-6} M + KNO_3 3 × 10^{-3} M and c) albumin + Barquat 4/1 + KNO_3 3 × 10^{-3} M (×5)*

TABLE 1

Possible main vibrational frequencies of FT-Raman spectrum of Barquat – 80, FT-SERS on Ag colloid, FT-SERS on mixed colloid and Raman spectra on Ag colloid

FT-Raman Spectrum of Barquat-80	FT-SERS on Ag-colloid (A)	FT-SERS on mixed colloid (B)	Raman spectrum on Ag colloid ©	Assignments
3064 cm^{-1} (s)	3058 cm^{-1} (m)	3073 cm^{-1} (m)		Aromatic C-H stretch
2953 ´´ (sh)	2968 ´´ (sh)			$-CH_3$ anti-symmetric stretch or methyl. C-H assym or symm stretch
2931 ´´ (sh)	2931 ´´ (s)	2938 ´´ (m)		$-CH_3$ anti-symmetric stretch
2891 ´´ (s)				$-CH_2$ symmetric stretch or methane C-H stretch
2852 ´´ (vs)	2848 ´´ (sh)	2856 ´´ (sh)		$-CH_2$ symmetric stretch
1605 ´´ (m)	1605 ´´ (w)	1632 ´´ (w)		Aromatic v (C-C)
1448 ´´ (s)	1443 ´´ (w)	1448 ´´ (m)	1456-1453 cm^{-1} (w)	$-CH_3$ anti-symmetric stretch or methyl C-H assym or symm stretch
1381 ´´ (w)	1386 ´´ (w)	1400 ´´ (w)		$-CH_3$ symmetric deformation or methyl C-H assym or symm stretch
	1324 ´´ (sh)		1318 ´´ (vw)	-CH methine deform
1302 ´´ (m)	1282 ´´ (vw)	1295-1305 ´´ (wv)	1292 ´´ (vw)	-CH methine deform or δip (arom C-H)
1032 ´´ (m)	1032 ´´ (w)	1032 ´´ (w)	1039 ´´ (m)	Aromatic C-H in-plane def. or methine skeletal C-C vib
1004 ´´ (s)	1004 ´´ (m)	1004 ´´ (m)	1003 ´´ (s)	Aromatic C-H in-plane def. or methine skeletal C-C vib or amines v_{C-N}
873 – 888 ´´ (w)			870 ´´ (w)	Aromatic δ_{oop}(C-H) or methine skeletal C-C vib.
837 ´´ (w)	839 ´´ (w)	837 ´´ (w)	836 ´´ (w)	Aromatic δ_{oop} (C-H)
784 ´´ (vw)			783 ´´ (vw)	Aromatic δ_{oop} (C-H) or methine skeletal C-C vib
732 ´´ (w)	727 ´´ (vw)	735 ´´ (vw)	737-724 ´´ (w)	Aromatic δ_{oop} (C-H) or $-(CH_2)_n-$ sim δ (C-H)
620 ´´ (w)			619 ´´ (w)	

TABLE 2

SERS: a) Albumin 2.8 × 10^{-5} M + KNO_3 3 × 10^{-3} M (x5); b) barquat 7 × 10^{-6} M + KNO_3 3 × 10^{-3} M and c) albumin + Barquat 4/1 + KNO_3 3 × 10^{-3} M (x5)

Albumin 2.8 × 10^{-5} M + KNO_3 3 × 10^{-3} M (x5)	Barquat 7 × 10^{-6} M + KNO_3 3 × 10^{-3} M	Albumin + Barquat (4/1) + KNO_3 3 × 10^{-3} M	Assignements
3209 cm^{-1} (s)(br)	3211 cm^{-1} (s)(br)	3213 cm^{-1} (s)(br)	
3060 ´´ (sh)	3060 ´´ (m)	3052 ´´ (w)	Aromatic C-H stretch
	2969 ´´ (sh)		Alkanes v (C-H)
2932 ´´ (m)	2926 ´´ (m)	2927 ´´ (s)	$-CH_3$ anti-symmetric stretching or Alkanes v (C-H)
	2892 ´´ (sh)		$-CH_3$ anti-symmetric stretching or Alkanes v (C-H)
1645 ´´ (s)	1645 ´´ (m)	1647 ´´ (s)	Amines δ_{NH}
	1604 ´´ (w)	1600 ´´ (vw)	Aromatic v (C-C)
1572 ´´ (vw)		1576 ´´ (m)	Aromatic v (C-C) or amines δ_{NH}
1540 ´´ (vw)		1532 ´´ (w)	Aromatic v (C=C)
	1437 ´´ (m)	1438 ´´ (sh)	$-CH_3$ $\delta_{C\text{-}H\ asim}$
1378 ´´ (s)	1382 ´´ (w)	1386 ´´ (s)	$-CH_3$ $\delta_{C\text{-}H\ asim}$
1293 ´´ (m)	1299 ´´ (m)	1295 ´´ (m)	Aminas v (C-N)
	1216 ´´ (w)		Aminas v (C-N)
1190 ´´ (m)	1191 ´´ (w)	1191 ´´ (s)	Aminas v (C-N)
	1127 ´´ (w)	1127 ´´ (vw)	(-C-C-) stretching or δ(C-H) aromatic
	1083 ´´ (w)	1075 ´´ (w)	Aromatic δ_{ip} (C-H)
1031 ´´ (s)	1031 ´´ (s)	1030 ´´ (s)	Aromatic C-H in-plane def. or methane skeletal C-C vib
1003 ´´ (sh)	1003 ´´ (s)	1003 ´´ (s)	Aromatic C-H in-plane def. or methane skeletal C-C vib. or amines $v_{C\text{-}N}$
948 ´´ (s)	948 ´´ (s)	949 ´´ (s)	Aromatic δ_{ip} (C-H)
831 ´´ (m)	837 ´´ (s)	837 ´´ (s)	Aromatic δ_{oop} (C-H)
802 ´´ (m)		790 ´´ (m)	Aromatic δ_{oop} (C-H)
736 ´´ (w)	734 ´´ (m)	730 ´´ (m)	Aromatic δ_{oop} (C-H)
	620 ´´ (m)		

(medium) in Barquat assigned to aromatic δoop (C-H), possible are observed at 730 cm^{-1} (medium). All these peaks point that the interaction with HSA and Barquat is also on the aromatic ring.

CONCLUSION

SERS of Barquat–80 using mixed colloids shows the increase of the numeral values of spectrum owing to the presence of two metallic ions: Ag^+ and Fe^{3+} and the profile of spectrum indicates that N^+ of the molecule of Barquat–80 is fixed over the surface that has positive electric charge and its molecular structure determines that the aromatic ring and the $-CH_3$ radicals are placed next the metallic surface, but the paraffinic chain is placed far the surface. The presence of NaCl increases to fix the molecule on the surface. The higher values of FT-SERS spectra over magnetic colloid than over silver colloid possible is due to more intense interaction between molecule of Barquat–80 and the metallic surface. The more intense spectrum of Barquat over C colloid points that the molecule is absorbed with more force on this colloid, only the bands that correspond to vibrations of benzene point that the interaction of this radical with C colloid is weaker than in the others colloids. The interaction between Barquat – 80 and albumin looks in the spectrum because the intensity is lower in the mixture that in the Barquat–80 and this molecule joined to albumin by alkane chain and $-CH_3$ or $-CH_2$ radicals and with a noteworthy interaction of the aromatic points.

REFERENCES

1. Lonza group information.
2. Kuca K, Marek J, Stodulka P, et al. Preparation of benzalkonium salts differing in the length of a side alkyl chain. Molecules. 2007;12:2341-7.
3. Pescina S, Carra F, Padula C, et al. Effect of pH and penetration enhancers on cysteamine stability and trans-corneal transport. Eur J Pharm Biopharm. 2016;107:171-9.
4. Lin Z, He H, Zhou T, et al. A mouse model of limbal stem cell deficiency induced by topical medication with the preservative benzalkonium chloride. Invest Ophtalmol Vis Sci. 2013;54:6314-25.
5. Sunada A, Kimura K, Nishi I, et al. *In vitro* evaluations of topical agents to treat acanthamoeba keratitis. Ophtalmology. 2014;121:2059-65.
6. Chen W, Zhang Z, Hu J, et al. Changes in rabbit corneal innervation induced by the topical application of benzalkonium chloride. Cornea. 2013;32:1599-606.
7. Torhildsen G, Frisk S, Bai M, et al. Safety and comfort evaluation of a new formulation of Visine® lubricant eye drops containing HydroBlend™ and GentlePur™ Clin Ophthalmol. 2016;10:331-6.
8. González-Andrades M, Carriel V, Rivera-Izquierdo M, et al. Effects of detergent-based protocols on decellularization of corneas with sclerocorneal limbus. Evaluation of regional differences. Trans Vis Sci Technol. 2015;4:13.
9. Mazzoni A, Tjaderhane V, Checchi R, et al. Role of Dentin MMPs in caries progression and bond stability. J Dent Res. 2015;94:241-51.
10. Bridier A, Briandet R, Thomas V, et al. Comparative biocidal activity of peracetic acid, benzalkonium chloride and ortho-phthalaldehyde on 77 bacterial strains. J Hosp Infect. 2011;78:208-13.
11. Ioannou CJ, Hannlon GW, Denyer SP. Action of disinfectant quaternary ammonium compounds against *Staphylococcus aureus*. Antimicrob Agents Chemother. 2007;51:296-306.
12. Biergbaek LA, Haagensen JAJ, Molin S, et al. Effect of oxygen limitation and starvation on the benzalkonium chloride susceptibility of *Escherichia coli*. J App Microbiol. 2008;105:1310-7.
13. Zakrajseĕk J, Stoji V, Bohanec S, et al. Quality by design based optimization of a high performance liquid chromatography method for assay determination of low concentration preservatives in complex nasal formulations. Acta Chim Slov. 2015;62:72-82.
14. Patarca R, Rosenzweig JA, Zuniga AA, et al. Benzalkonium salts: Effects on G-protein-mediated processes and surface membranes. Crit Rev Oncol. 2000;11:225.
15. Khan AH, Top E, Scott A, et al. Biodegradation of benzalkonium chlorides singly and in mixtures by a *Pseudomonas* sp. isolated from returned activated sludge. J Hazard Mater. 2015;299:595-602.
16. Brycki B, Malecka I, Koziroq A, et al. Synthesis, structure and antimicrobial properties of novel benzalkonium chloride analogues with pyridine rings. Molecules. 2017;22:130.

17. Jain P, Chakma B, Singh N, et al. Aromatic surfactant as aggregating agent for aptamer-gold nanoparticle-based detection of plasmodium lactate dehydrogenase Mol Biotechnol. 2016;58:497-508.
18. Araújo PA, Merglhão F, Melo L, et al. The ability of an antimicrobial agent to penetrate a biofilm is not correlated with its killing or removal efficiency. Biofouling. 2014;30:675-83.
19. Tandukar M, Tezel S, Konstantinidis KT, et al. Long-term exposure to benzalkonium chloride disinfectants results in change of microbial community structure and increased antimicrobial resistance. Environ Sci Technol. 2013;47:9730-8.
20. Lukáš M, Mrva M, Garajová M, et al. Synthesis, self-aggregation and biological properties of alkylphosphocholine and alkylphosphohomocholine derivatives of cetyltrimethylammonium bromide, cetylpyridinium bromide, benzalkonium bromide (C16) and benzethonium chloride. Eur J Med Chem. 2013;66:46-55.
21. Noecker R, Miller KV. Benzalkonium chloride in glaucoma medications. Ocul. Surf. 2011;9:159-62.
22. Chen W, Li Z, Hu J, et al. Corneal alternations induced by topical application of benzalkonium chloride in rabbit. PLoS One. 2011;6:26103.
23. Nagai N, Yoshioka C, Tanino T, et al. Decrease in corneal damage due to benzalkonium chloride by the addition of mannitol into timolol maleate eye drops oleo. Science. 2015;64:743-50.
24. Nagai N, Ito Y, Okamoto N, et al. Comparison of the enhancement of plasma glucose levels in type 2 diabetes Otsuka Long-Evans Tokushima fatty rats by oral administration of sucrose or maple syrup. J Oleo Sci. 2013;62: 737-43.
25. Beaudouin C, Labbe A, Liang H, et al. Preservatives in eye drops: The good, the bad and the ugly. Progr Retinal Eye Res. 2010;29:312-34.
26. Beaudouin C. Detrimental effect of preservatives in eye drops: Implications for the treatment of glaucoma. Acta Opthalmol. 2008;86:716-26.
27. Simonetti S, Díaz-compañiy A, Brizuela G, et al. β-cristobalite (001) surface as 4-formaminoantipyrine adsorbent: First principle study of the effect on adsorption of surface modification. Colloids Surfaces B Biointerfaces. 2016;148:287-92.
28. Le Ru EC, Etchegoin PG. Principles of surface-enhanced Raman spectroscopy and related plasmonic effects. (1st ed.) Elsevier, Amsterdam. 2008.
29. Zeng Z, Liu Y, Wei J. Recent advances in surface-enhanced Raman spectroscopy (SERS): Finite-difference time-domain (FDTD) method for SERS and sensing applications. Trans Trends Anal Chem. 2016;75:162-73.
30. Stiles PL, Dieringer JA, Shah NC, et al. Surface-enhanced Raman spectroscopy. Annu Rev Anal Chem. 2011;1:601-26.
31. Muniz-Miranda M, Gellini C, Giorgetti E. Surface-enhanced Raman scattering from copper nanoparticles obtained by laser ablation. J Phys Chem. 2011;115:5021-7.
32. Stiufiuc R, Iacovita C, Lucaciu CM, et al. SERS-active silver colloids prepared by reduction of silver nitrate with short-chain polyethylene glicol. Nanoscale Res Lett. 2013;8:47.
33. http://en.wikipedia.org/Wiki/Surface_enhanced_Raman_spectroscopy
34. Xiao C, Chen Z, Zhang D, et al. Research on the temperature effect characteristics of SERS enhancement factor. Optik. 2016;127:9926-31.
35. Sharma B, Fernández Cardinal M, Kleinman SL, et al. High-performance SERS substrates: Advances and challenges. M R S Bull. 2013;38:615-24.
36. Hurtadoa RB, Valadezb MC, Ramírez-Rodríguez LP, et al. Instant synthesis of gold nanoparticles at room temperature and SERS applications. Phys Lett A. 2016;380:2658-63.
37. Liu H, Yang L, Liu J. Three-dimensional SERS hot spots for chemical sensing: Towards developing a practical analyzer. Trends Anal Chem. 2016;80:364-72.
38. Lehninger AL, Nelson DL, Coc MN. Principios de Bioquímica Ediciones Omega Barcelona 1995.
39. Ghuman J, Zunszain PA, Petitpas I, et al. Structural basis of the drug-binding specificity of human serum albumin. J Mol Biol. 2005;353:38-52.
40. Hein KL, Kragh-Hansenet U, Preben Morth J, et al. Crystallographic analysis reveals a unique lidocaine binding site on human serum albumin. J Struct Biol. 2010;171:353-60.
41. Hashimoto S, Yabusaki T, Takeuchi H, et al. Structure and ligand binding modes of human serum albumin studied by UV resonance Raman spectroscopy. Biospectroscopy. 1995;1:375 -85.
42. Miskovsky P, Hritz, J, Sánchez–Cortés S, et al. Interaction of hypericin with serum albumins: Surface enhanced Raman spectroscopy, resonance Raman spectroscopy and molecular modeling study. Photochem Photobiol. 2001;74:172-83.
43. Tamion F. Annales francaises d´anesthesie et de Reanimation. 2010;29:629-34.
44. Carter DC, He XM, Munson SH, et al. Three-dimensional structure of human serum albumin. Science. 1989;244:1195-8.
45. Cao LH, Sun LH, Liu L, et al. Structural consistency analysis of recombinant and wild-type human serum albumin. J Mol Struct. 2017;1127:1-5.
46. Lee DC, Meisel D. Adsorption and surface-enhanced raman of dyes on silver and gold sols. J Phys Chem. 1982;84:3391-5.
47. Massart, R. Preparation of aqueous magnetic liquids in alkaline and acidic media. Trans Magnetics. 1981;17:1247-8.
48. Leopold N, Lendl B. A new method for fast preparation of highly surface-enhanced Raman scattering (SERS) active silver colloids at room temperature by reduction of silver nitrate with hydroxylamine hydrochloride. J Phys Chem. 2003;107:5723-7.